Future Sustainability
Open Access Journal
ISSN 2995-0473

May 2024| Volume 02 | Issue 02 | Pages 08-19

Journal homepage: https://fupubco.com/fusus

https://doi.org/10.55670/fpll.fusus.2.2.2

Future Publishing LLC

Review

Advancements in machine learning for predicting phases in high-entropy alloys: a comprehensive review

MD. Tanvir Amin*, Wahid Bin Noor
Department of Mechanical Engineering, Chittagong University of Engineering and Technology, Bangladesh

ARTICLE INFO

Article history:
Received 03 December 2023
Received in revised form
02 January 2024
Accepted 09 January 2024

Keywords:
High-entropy alloys, Machine learning, Phase prediction, Dataset optimization, Model evaluation, Feature analysis

*Corresponding author
Email address:
u1903021@student.cuet.ac.bd

DOI: 10.55670/fpll.fusus.2.2.2

ABSTRACT

High entropy alloys (HEAs) are distinguished by their enhanced physicochemical properties, attributed to the formation of various phases such as solid solution (SS), intermetallic (IM), or a combination (SS + IM). These phases contribute distinctively to the microstructure of the alloys. A critical aspect of alloy design revolves around accurately predicting these phases, which has led to the integration of sophisticated data vetting methods and Machine Learning (ML) algorithms in recent research. This review paper aims to provide a comprehensive analysis of the advancements in phase prediction accuracy within HEAs, an essential component in the development of these alloys. HEAs are known for their intricate compositions, offering a wide spectrum of material properties, making them particularly relevant for applications aimed at future sustainability. Phase engineering in HEAs unlocks the potential for creating materials tailored to eco-friendly technologies and energy-efficient solutions. The challenge in predicting phase selection in HEAs is accentuated by the limited data available on these complex materials. This review delves into how advanced data vetting techniques and ML algorithms are being employed to overcome these challenges, thus contributing significantly to sustainable material design. The paper examines various algorithms used in HEA phase prediction, including KNN (K-Nearest Neighbors), SVM (Support Vector Machines), ANN (Artificial Neural Networks), GNB (Gaussian Naive Bayes), and RF (Random Forest). It discusses the testing accuracy of these algorithms in classifying HEA phases, revealing variations in their effectiveness. The review highlights the superior accuracy of ANNs, followed closely by KNN and SVM, while noting the comparatively lower accuracy of GNB. This comprehensive review synthesizes current research efforts in utilizing computational methods to design HEAs, underlining their broader implications in expediting the discovery and development of diverse metal alloys. These efforts are pivotal in meeting the evolving demands of modern engineering applications, thereby contributing to the advancement of materials science.

1. Introduction

Machine Learning (ML) represents a comprehensive category of data-driven algorithms designed for the purpose of deriving inferences and making classifications based on meticulously observed data. These algorithms demonstrate a unique capacity for iterative refinement, allowing them to glean concealed insights from heterogeneous, complex, and high-dimensional datasets, all achieved without the requirement for explicit programming [1]. Machine Learning (ML) has evolved into an essential technology underpinning a myriad of real-world applications, with its pervasive impact extending notably into domains such as material informatics [1, 2]. The efficacy of machine learning extends to achieving superlative outcomes across diverse domains, including

strategic applications like board game mastery (e.g., Go [3]), autonomous vehicular navigation [4], and image classification [5]. Consequently, substantial segments of our daily lives, encompassing pivotal domains such as visual and auditory recognition [6], online searches [7], email/spam filtration [8], credit scoring [9], and more, rely significantly on the sophisticated capabilities inherent in machine learning algorithms (Figure 1). Metal alloys have been instrumental throughout world history, with their significance dating from the historical period known as the Bronze Age. In the modern era, these alloys assume critical roles in diverse applications within automotive and aerospace engineering industries [11], as well as serving as fundamental materials in nuclear and biomedical contexts [12]. High entropy alloys (HEAs), commonly known as Multi-Principal Element Alloys (MPEAs), are alloys characterized by the inclusion of a minimum of five principal elements. Each principal element is distinguished by a composition surpassing the threshold of 5% [13]. The initial characterization provided represents the foundational definition of High Entropy Alloys (HEAs). However, an alternate viewpoint has been put forth by certain researchers, suggesting that HEAs may be constituted by four equi-atomic elements [14-17]. HEAs (Figure 2) have attracted considerable attention owing to their elevated strength, superior mechanical properties, and unexplored possibilities within alloy compositions, rendering them a subject of broad scholarly interest [18-28]. High-entropy alloys (HEAs) have garnered substantial attention owing to their distinctive properties, a phenomenon largely contingent upon the deliberate selection among three discernible phases: solid solution (SS), intermetallic compound (IM), and the coexistence of solid solution and intermetallic compound (SS & IM) [29].

The surge in machine learning applications within the domain of material science is experiencing exponential growth. The ensuing discussion highlights notable recent contributions in employing machine learning methodologies for the study of High-Entropy Alloys (HEAs). Islam et al. [31] categorized High-Entropy Alloys (HEAs) into Solid Solution, Amorphous, and Intermetallic categories utilizing a Neural Network algorithm, incorporating five features as input variables. The reported results include a training accuracy of 99% and an average cross-validation accuracy (4-fold) of 83%. Huang et al. [29] performed phase classification on Miracle et al.'s [32] High-Entropy Alloy (HEA) dataset employing three distinct algorithms: Support Vector Machine (SVM), Artificial Neural Network (ANN) and K-Nearest Neighbor (KNN). In these investigations, a set of five input features was employed for the three-phase classification. The most favorable outcomes were documented as 64.3%, 74.3%, and 68.6% for SVM, ANN, and KNN, respectively, underscoring the superiority of ANN as the optimal classification algorithm. Agarwal et al. [33] employed an Adaptive Neuro-Fuzzy Interface System (ANFIS) machine learning algorithm to classify High-Entropy Alloy (HEA) phases, including FCC, BCC, and Other Multiphases. The study conducted a comparative assessment between two models: one predicated on the composition of elements as inputs and the other based on thermodynamic parameters. Results revealed that the composition-based model exhibited a notable accuracy of 84.1%, surpassing the parameter-based approach, which achieved an accuracy of 80%. Consequently, the investigation concluded that, in this context, the input derived from compositional elements proved to be more effective for the classification of HEAs.

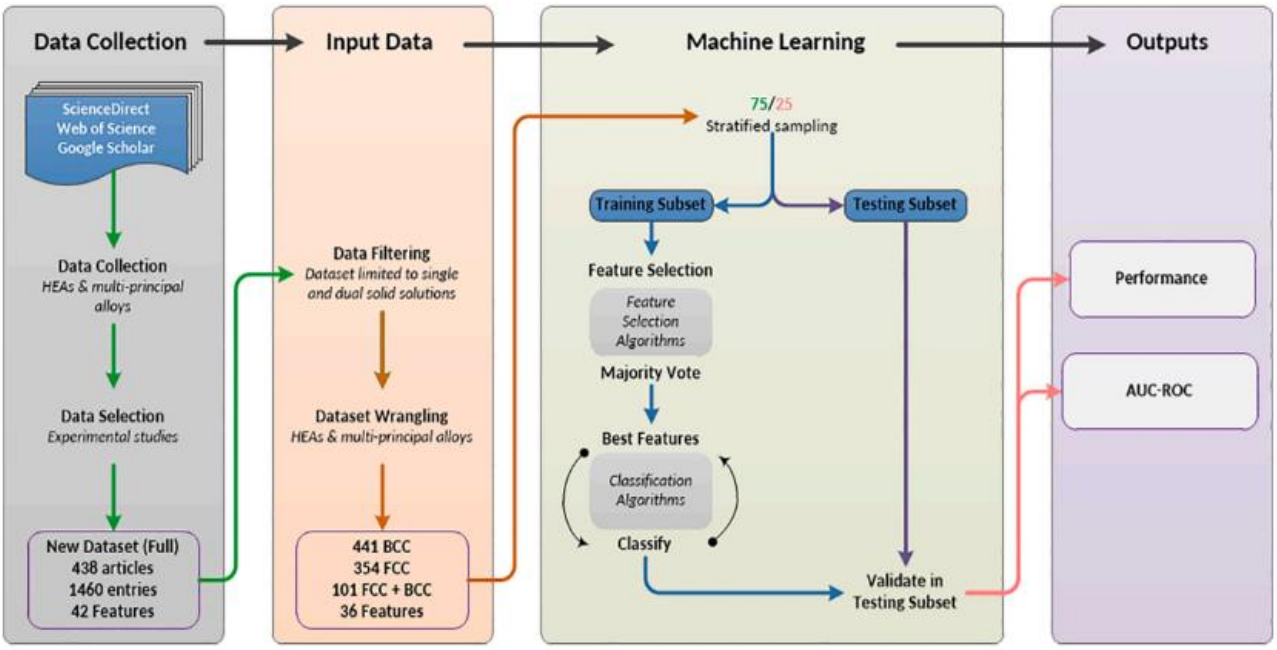

Figure 1. ML modeling framework for phase classification developed specifically for this study [10]

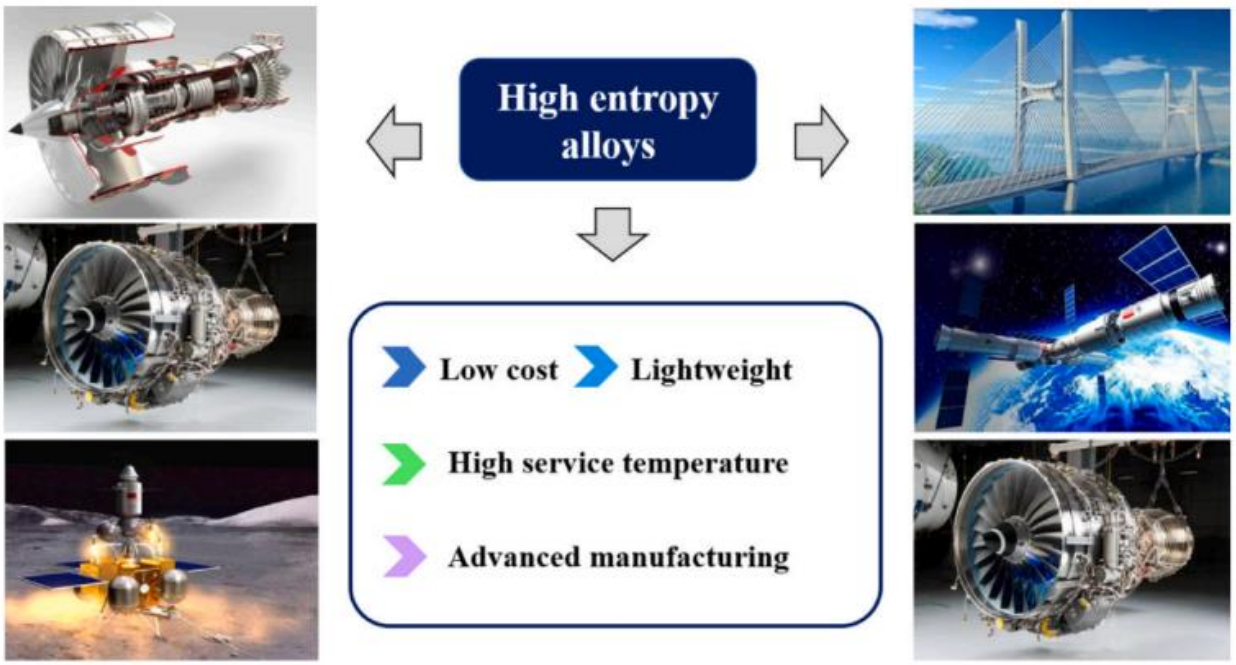

Figure 2. Pressing demand for high entropy alloys [30]

Zhou et al. [34] applied three distinct machine learning algorithms— Convolutional Neural Network (CNN), Support Vector Machines (SVM) and Artificial Neural Network (ANN)—to predict phases (SS, IM, and AM) in High-Entropy Alloys (HEAs). The feature set comprised 13 parameters, encompassing Atomic Size Difference, Average and SD of Bulk Modulus, Average and SD of Electronegativity, Average and SD of Mixing Enthalpy, Mean Atomic Radius, Average and SD of Valence Electron Concentration (VEC), Ideal Mixing Entropy and Average and Standard Deviation (SD) of Melting Temperatures. The study also implemented a feature reduction technique, revealing that the model with reduced features performed sub-optimally compared to the one utilizing the complete feature set. R. Machaka [10] conducted an evaluation of two machine learning algorithms, namely Random Forest and Decision Tree, for the classification of phases in High-Entropy Alloys (HEAs)—specifically BCC SS, FCC SS, FCC + BCC SS, and IM. The input feature set encompassed five features. The results demonstrate that Random Forest outperformed Decision Tree in phase classification, achieving a noteworthy test accuracy of 82.3%. It is essential to recognize that each algorithm exhibits unique features and distinctive advantages. In the context of this research, prioritizing parameter independence, three widely recognized machine learning algorithms—namely, (1) Support Vector Machines (SVM), (2) Artificial Neural Network (ANN), and (3) K-nearest neighbors (KNN)—have been implemented to anticipate phase selection within High-Entropy Alloys (HEAs), encompassing the IM, SS, and SS + IM phases. The overarching aim is to discern the most appropriate machine learning model for the prospective design and discovery of new HEAs [29].

2. Literature review

2.1 Current state of research in high-entropy alloys

The field of High-Entropy Alloys (HEAs) has been an active area of research, and it's essential to note that advancements may have occurred since then. The current state of research in high-energy alloys (HEAs) is characterized by a dynamic exploration of novel compositions and advanced processing techniques. Researchers are broadening the applications of HEAs across industries, focusing on tailoring properties for specific needs. The field emphasizes understanding phase stability, employing computational modeling for predictive design, and optimizing multifunctional capabilities. Collaborative efforts on an international scale drive knowledge exchange, while challenges, including processing scalability and environmental considerations, present opportunities for innovation. Ongoing research aims to unlock the full potential of HEAs by addressing these challenges and further advancing their applications in diverse and sustainable materials science domains.

2.2 Machine learning in material science

Machine learning (ML) is assuming a growing role within our society, particularly in the domains of materials science and engineering [35]. Machine Learning (ML) has emerged as a transformative force in the realm of Material Science, fundamentally altering the landscape of material discovery, design, and characterization. ML methodologies facilitate precise prediction and optimization of material properties, offering high-throughput screening capabilities for extensive databases and contributing significantly to the burgeoning field of materials informatics. Its application spans crystal structure prediction, the acceleration of simulation and modeling processes, and the automated analysis of material microstructures through advanced image analysis. ML plays a

pivotal role in predicting material failure modes, evaluating durability, and optimizing experimental design strategies. Beyond these applications, ML aids in the discovery of novel materials classes, guiding researchers towards unexplored compositions with unique properties. The integration of ML with quantum computing further refines the accuracy of simulations at the quantum level. The symbiosis between ML and Material Science stands as a driving force, enhancing research efficiency and fostering innovation in the pursuit of materials with unprecedented and tailored properties.

3. Methodology

3.1 KNN

The algorithm named K-Nearest Neighbors (KNN) is a machine learning approach employed in high entropy alloy (HEA) phase prediction. In the context of HEAs, KNN operates by identifying the phases of interest based on the similarity of their composition to neighboring data points in a feature space. The K-nearest neighbors (KNN) algorithm is a widely adopted non-parametric supervised learning approach employed to address both regression and classification problems [25- 27]. In the realm of classification problems, the training dataset, characterized by vectors within an n-dimensional space (where n is set to 5, reflecting the five input features), is systematically assigned distinct labels. In the subsequent testing phase, a testing data vector is introduced into the space, and the Euclidean distance algorithm is applied to determine the distances between this testing vector and the training vectors [39].

$$d(\boldsymbol{p},\boldsymbol{q}) = d(\boldsymbol{q},\boldsymbol{p}) = \sqrt{\sum_{i=1}^{n}(q_i - p_i)^2} \quad (1)$$

Where $\boldsymbol{p} = (p_1, p_2, \dots\dots, p_n)$ represents the testing vectors and $\boldsymbol{q} = (q_1, q_2, \dots\dots, q_n)$ is one of the KNN training vectors. The algorithm classifies an unknown alloy phase by assessing the classes of its k-nearest neighbors in the training dataset, where "k" is a predefined number of neighboring data points. The distance metric, often Euclidean distance, is employed to quantify the resemblance between the unknown alloy and its neighbors. KNN is particularly effective when the underlying structure of the dataset exhibits distinct clusters or regions corresponding to different phases. This algorithm is versatile and straightforward to implement, making it a valuable tool for phase prediction in high entropy alloy research.

3.2 SVM

Support Vector Machines (SVM) is a potent machine learning algorithm applicable to diverse tasks, including high entropy phase prediction in materials science. Utilizing a labeled dataset comprising samples with known phase labels, SVM operates through feature extraction, identifying relevant properties such as atomic compositions or lattice parameters indicative of a material's phase. Trained on this dataset, the algorithm seeks the optimal hyperplane in feature space to separate different classes, maximizing the margin while minimizing errors. The trained SVM model can then predict the phase of new, unseen high-entropy materials by assigning class labels based on their positions relative to the learned hyperplane. The hyperparameters employed in Support Vector Machines (SVM) encompass kernel function, kernel coefficient (γ) and the penalty parameter (C). The parameter C functions as a regularization factor, governing the classifier's propensity to avoid misclassification of training examples. A higher C value facilitates a more inclusive classification of training set examples; nevertheless, an excessively elevated C may induce overfitting, compromising the model's capacity to generalize to new data. Conversely, a diminutive C may result in inadequate accommodation of outliers, leading to substantial errors in the training set. The kernel function plays a pivotal role in defining the feature domain for classification, with the SVM method utilizing it to calculate the distance between feature vectors [40]. Nonlinear training samples (Figure 3) within an input space can be transformed into a feature domain using algorithm $\boldsymbol{\Theta}$. This algorithm constructs a hyperplane Γ, typically in a dimension denoted as R^{N-1}, utilizes an optimal margin for effective classification between two distinct categories [41]. $\boldsymbol{\Theta}$ (x_i) then replaces each training pattern x_i and executes the optimal hyperplane algorithm within the feature space. The definition of a kernel function is as follows:

$$k(\boldsymbol{x},\boldsymbol{y}) = (\boldsymbol{\Theta}(\mathbf{x}).\boldsymbol{\Theta}(\mathbf{y})) \quad (2)$$

From Equation, it is evident that a higher dimension in the feature domain corresponds to a more intricate kernel function. The choice of different kernel functions results in distinct algorithms, including Gaussian, polynomial and radial basis function [42].

The Gaussian kernel, a frequently employed kernel method, is recognized for its ability to achieve a nuanced and precise balance between fitting and smoothing data. Consequently, in the context of this study, we have chosen to utilize the Gaussian kernel. In spaces of one, two, and N dimensions, the Gaussian kernel function is formally defined as [43]:

$$G_{1D}(x,\sigma) = \frac{1}{\sigma\sqrt{2\pi}}\ exp\left(-\frac{x^2}{2\sigma^2}\right) \quad (3)$$

$$G_{2D}(x,y,\sigma) = \frac{1}{2\pi\sigma^2}\ exp\left(-\frac{x^2+y^2}{2\sigma^2}\right) \quad (4)$$

$$G_{ND}(\boldsymbol{x},\sigma) = \frac{1}{(\sigma\sqrt{2\pi})^N}\ exp\left(-\frac{\|x\|^2}{2\sigma^2}\right) \quad (5)$$

respectively where σ, the standard deviation, sets the scale parameter of the Gaussian function and σ^2 is known as the variance.

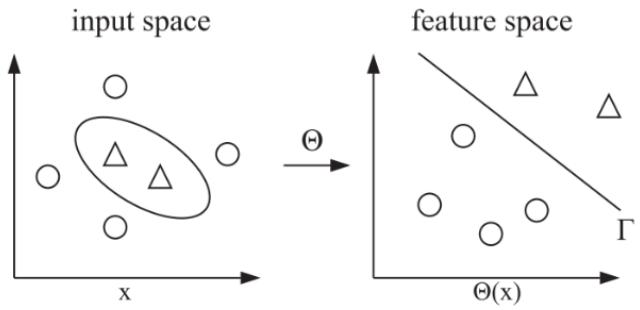

Figure 3. A diagram illustrating the nonlinearity inherent in a classification problem with support vector machines is converted into a linear problem by employing a kernel function **Θ**. This transformation results in the definition of a plane Γ, referred to as a hyperplane, within the feature space [29]

3.3 ANN

Artificial Neural Networks (ANN) are a powerful machine learning algorithm employed for high entropy phase prediction, particularly in fields like materials science. Modeled after the human brain, ANNs comprise interconnected nodes arranged in layers. The Artificial Neural Network (ANN) is formulated as a network of interconnected artificial neurons, strategically structured to simulate the cognitive functions observed in a biological learning system, specifically mirroring aspects of the human brain [44]. The input layer receives features like atomic compositions, while intermediate hidden layers, with weighted connections between neurons, enable the network to capture intricate relationships. The output layer produces predictions for material phases, learning to assign probabilities to each phase. In the context of this study, two primary types of Artificial Neural Network (ANN) models are utilized: the supervised Multi-Layer Feed-Forward Neural Network (MLFFNN) and the unsupervised Self-Organizing Maps (SOMs).

3.3.1 SOM

The Kohonen Self-Organizing Map (SOM) method represents a conventional unsupervised machine learning neural network approach. In this method, the network autonomously learns to differentiate between groups without requiring prior knowledge of their labels [45]. The Self-Organizing Map (SOM) algorithm, employed for high entropy phase prediction, stands out as an unsupervised learning technique that excels in uncovering inherent patterns within complex datasets. Particularly valuable in materials science, the SOM algorithm organizes high entropy phases into a topological map, providing a visual representation of their relationships and similarities. By autonomously clustering and mapping the input data, SOMs offer insights into the intrinsic organization of materials without the need for labeled training data. This proves advantageous when dealing with intricate structures of high entropy phases, as the algorithm reveals emergent patterns that may not be immediately apparent. The SOM's ability to capture and visualize the underlying structure of multi-elemental compositions makes it a valuable tool for researchers seeking a holistic understanding of high entropy materials without relying on pre-defined labels (Figure 4).

3.3.2 MLFFNN

The algorithm known as Multi-Layer Feed-Forward Neural Network (MLFFNN) is applied for high entropy alloy (HEA) phase prediction in a supervised learning framework. In the framework of a Multi-Layer Feed-Forward Neural Network (MLFFNN) [46], the neurons are compelled to establish connections in the onward direction. The architectural configuration of the neural network constitutes the foundational step in the construction of the Multi-Layer Feed-Forward Neural Network (MLFFNN). The critical decision involves defining the number of hidden layers, wherein an augmentation of hidden layers is conventionally associated with heightened processing time and an expanded storage demand for learning parameters. It has been discerned that a neural network architecture featuring merely two hidden layers proves inadequate for resolving intricate ternary classification problems, manifesting in an anticipated reduction in testing accuracy. Furthermore, we evaluate Neural network models employing four or more hidden layers in an MLFFNN architecture, revealing comparable accuracy levels albeit with a notable increase in computational demands. In order to strike a balance between testing accuracy and computational cost, our focus is directed towards utilizing three hidden layers in this work. The MLFFNN architecture, delineated in Figure 5, comprises an input layer, three hidden layers, and one output layer. The input layer serves as a conduit for external information, necessitating no further processing. The linear operation of the input feature vector is facilitated by a weight matrix, producing a new vector combined with a bias vector. Subsequently, an activation function assigned to each neuron in the initial hidden layer processes this resultant vector, and this iterative the procedure persists until the activation of the ultimate hidden layer, culminating in the formation of the output layer. The significance of the hidden layers lies in their capacity to learn the nonlinearity inherent in a problem and contribute decisively to its resolution, rendering them integral components of the overall network [29].

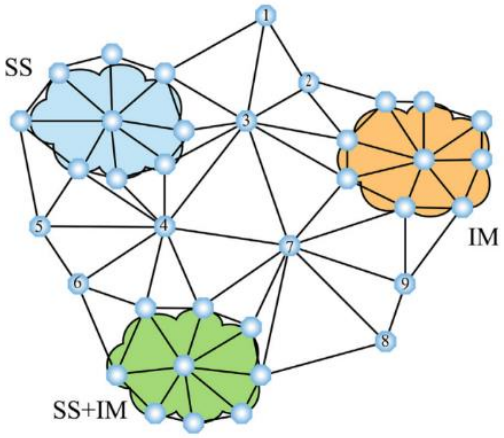

Figure 4. Three distinct groups exhibit well-defined spatial boundaries, and the "map" is designed to allocate groups of neurons for the explicit representation of each category. Simultaneously, residual neurons delineate an isolation band among the three groups

3.4 GNB

Gaussian Naive Bayes (GNB) is employed as a classification model for the purpose of estimating the phases within High Entropy Alloys (HEAs). The method operates under the assumption that each characteristic is assumed to be independent and follow a Gaussian distribution, employing Bayes' theorem [47]. The GNB classifier, using this Equation and a Gaussian probability density function, computes the posterior probability $P(X|Y)$ of each class when given a feature vector.

$$P(X_i|Y) = \frac{1}{\sqrt{2\pi\sigma^2_{Y,i}}}\, exp\left(-\frac{(X_i-\mu_{Y,i})^2}{2\sigma^2_{Y,i}}\right) \quad (6)$$

where X_i is the i^{th} of the sample, $\mu_{Y,i}$ is the mean of the i^{th} attribute for class Y, $\sigma_{Y,i}$ is the standard deviation of the i^{th} attribute for class Y, and $P(X_i|Y)$ is the probability of observing the i^{th} attribute given class Y.

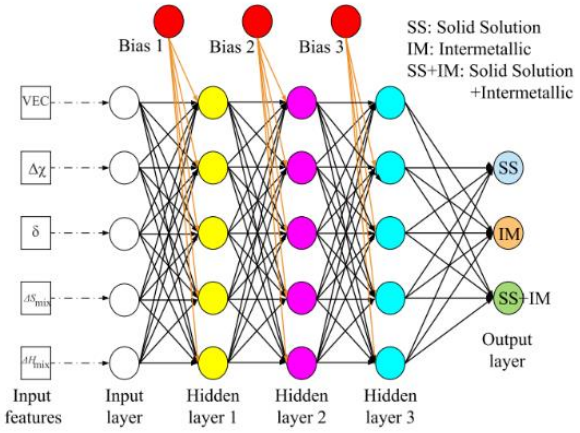

Figure 5. The architecture illustrates a multi-layer feed-forward artificial neural network, comprising an input layer, three hidden layers, and one output layer. The depiction includes the representation of five input features and three bias nodes.

During training, the algorithm estimates the mean and variance of features for each phase class, utilizing the independence assumption to simplify computations. When a new sample with feature values is presented, GNB calculates the probability of belonging to each phase class based on the learned parameters. The predicted outcome is then determined by selecting the class with the highest probability, serving as the anticipated high entropy phase. It is essential to recognize potential limitations, such as the sensitivity to the Gaussian assumption and the simplistic feature independence assumption, which may necessitate consideration of alternative models or more sophisticated approaches for complex high entropy systems [48].

3.5 RF

The Random Forest Classifier (RF) utilizes an ensemble of decision tree predictors, with each tree dependent on values from a randomly sampled vector. This vector is sampled independently and shares the same distribution across all trees within the forest, assuming the formation of n trees [39, 40]. The resultant prediction is computed by averaging the predictions of the individual trees. In classification, the predicted class is determined by the majority vote from the decision trees in the forest [51], as illustrated in Figure 6.

Let T represent the total number of trees in the forest and let $f_i(x)$ express the i-th tree's prediction for the input vector **x**. The RF model's prediction is subsequently furnished by.:

$$\hat{y}_i = \frac{1}{T}\sum t = 1^T f_t(x_i),\ x_i \in \mathcal{X} \quad (7)$$

where x_i represents the forecasted category for the sample, and $\mathcal{X}$ represents the entirety of input samples.

4. Result and Discussion

The assessment includes a detailed classification report table, a confusion matrix for a nuanced performance breakdown, and a receiver operating characteristic (ROC) analysis, providing insights into the model's discrimination capabilities. The KNN model, detailed in Table 1, demonstrates an overall accuracy of 0.81, excelling in precision for the IM and AM phases and recall for the SS and AM phases. Challenges arise in accurately identifying the SS+IM phase, reflected in the lowest F1-score. Despite comparable performance to other models, the KNN algorithm's computational demands may limit its practicality for extensive datasets. Additional insights into its performance are elucidated through the succinct presentation of the confusion matrix and ROC curve are mentioned in Figure 7(a) and Figure 7(b) respectively.

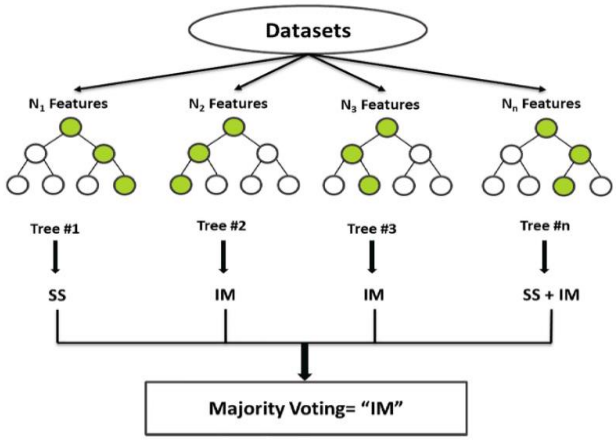

Figure 6. Operating principle of the Random Forest algorithm [52]

Table 1. Performance evaluation summary of the KNN model

Class	Precision	F1-Score	Recall	Support
SS	0.83	0.83	0.83	75
IM	0.93	0.83	0.74	77
AM	0.86	0.91	0.98	44
SS+IM	0.51	0.60	0.72	25
Accuracy	0.81			
Weighted Avg	0.84	0.82	0.81	221
Macro Avg	0.78	0.79	0.82	221

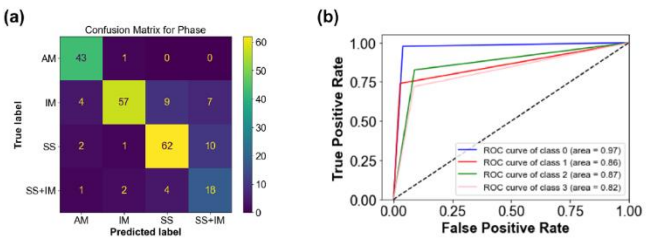

Figure 7. Assessment of the KNN classifier utilizing (a) Confusion matrix, and (b) Receiver Operating Characteristic (ROC) curve for multi-scale data [53]

The SVM model, outlined in Table 2, attains 81% overall accuracy, excelling with 98% recall and 86% precision for class AM but showing lower recall (56%) and precision (50%) for SS+IM phase. The macro-average F1 score of 0.77 indicates moderate overall performance, suggesting the SVM model's potential for dataset classification with performance variations across classes. Further analysis is necessary to assess robustness and generalizability, while visual aids such as the confusion matrix (Figure 8 (a)) and ROC curve (Figure 8 (b)) offer additional insights into the SVM model's performance.

Table 2. Performance evaluation summary of the SVM model

Class	Precision	F1-Score	Recall	Support
SS	0.83	0.81	0.79	75
IM	0.88	0.85	0.82	77
AM	0.86	0.91	0.98	44
SS+IM	0.50	0.53	0.56	25
Accuracy	0.81			
Weighted Avg	0.81	0.81	0.81	221
Macro Avg	0.77	0.77	0.79	221

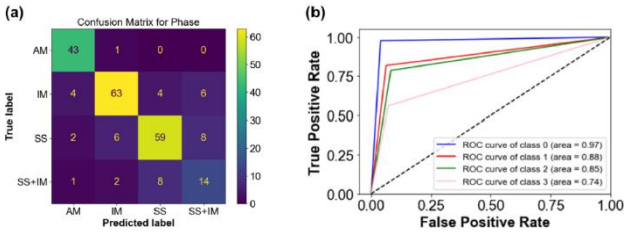

Figure 8. Assessment of the SVM classifier utilizing (a) Confusion matrix, and (b) Receiver Operating Characteristic (ROC) curve for multi-scale data [53]

We can see in Figure 9, In contrast to some studies that predominantly emphasize overall accuracy, it is equally imperative to underscore phase-wise accuracy for a comprehensive illustration of the model's competence in effectively predicting various phases. The results underscore the model's proficiency in accurately predicting distinct phases, with notable phase-wise accuracy levels: 81.25% for SS, 82.35% for IM and 86.67% for AM. These findings exemplify the effectiveness of the ANN model in predictive performance, particularly when trained on a balanced dataset for each phase. Employing Micro-F1 to assess the prediction outcomes, the test set is utilized to rigorously assess the effectiveness of the ANN model [54]. In the evaluation of the ANN model's predictive capabilities for each class of high-entropy alloys (HEA) within the dataset, a comprehensive examination was conducted. This involved the generation of a confusion matrix utilizing a testing dataset comprising 48 samples, as illustrated in Figure 10.

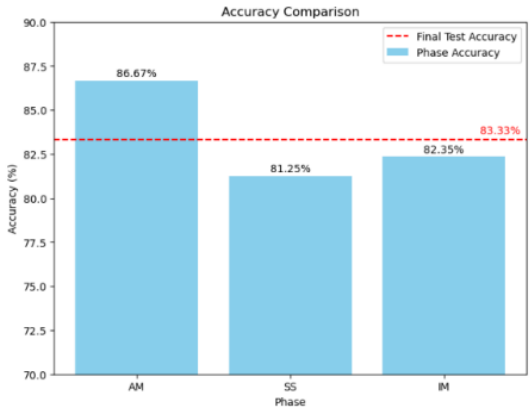

Figure 9. Evaluating phase-wise accuracy and overall average accuracy observed in the final test set [54]

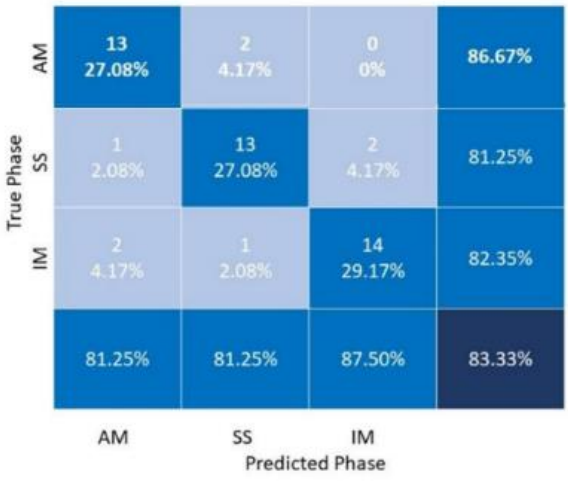

Figure 10. Confusion matrices depicting. The efficiency of the ANN model in predicting amorphous, solid solution, and intermetallic phases on the final test set [54]

The GNB model, detailed in Table 3, achieves an accuracy of 57% and a weighted F1 score of 0.59. Notably, it exhibits proficiency in estimating the SS and AM phases with precision scores of 0.79 and 0.82, respectively. However, challenges are observed in predicting the IM phase (moderate precision score of 0.71) and the SS+IM phase (precision score of 0.22), as outlined in the performance evaluation summary (Table 3). A concise evaluation is presented through a confusion matrix (Figure 11 (a)), depicting correct and incorrect classifications for each class, and a Receiver Operating Characteristic (ROC) curve (Figure 11 (b)), providing visual insights into the model's sensitivity and specificity.

The performance evaluation summary (Table 4) for the Random Forest (RF) model reveals an overall accuracy of 0.82, a marginal improvement over preceding model. The model performs exceptionally well in forecasting the IM and AM phases, demonstrating recall and precision scores of, 0.83 and 0.86 for IM and 0.95 and 0.91 for AM respectively. Similarly, commendable performance is noted in the SS phase with recall and precision scores of 0.83and 0.84. However,

challenges surface in predicting the SS+IM phase, evident in lower recall, F1 score and precision (0.52, 0.50, 0.48). The model's macro-average F1-score is 0.78, slightly below the SVM model, yet the weighted-average F1-score of 0.82 underscores its overall commendable performance. Complementary visual aids, comprising the confusion matrix (Figure 12 (a)) and ROC curve (Figure 12 (b)), offer additional insights into the subtle performance dynamics of the RF model.

Table 3. Performance evaluation summary of the GNB model

Class	Precision	F1-Score	Recall	Support
SS	0.79	0.50	0.36	75
IM	0.71	0.68	0.66	77
AM	0.82	0.76	0.70	44
SS+IM	0.22	0.33	0.68	25
Accuracy	0.57			
Weighted Avg	0.70	0.59	0.57	221
Macro Avg	0.63	0.57	0.60	221

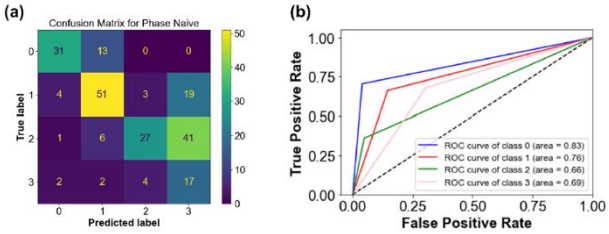

Figure 11. Assessment of the GNB classifier utilizing (a) Confusion matrix, and (b) Receiver Operating Characteristic (ROC) curve for multi-scale data [53]

Table 4. Performance evaluation summary of the RF model

Class	Precision	F1-Score	Recall	Support
SS	0.84	0.83	0.83	75
IM	0.86	0.85	0.83	77
AM	0.91	0.98	0.95	44
SS+IM	0.48	0.50	0.52	25
Accuracy	0.82			
Weighted Avg	0.82	0.82	0.82	221
Macro Avg	0.77	0.78	0.78	221

For hyperparameter optimization, various metrics were utilized to the validation dataset to assess the efficacy of machine learning models. Accuracy, Precision, F1 score, Recall, Zero-One loss, Log loss, hemming loss, Matthews Correlation Coefficient and Cohen-Kappa score were computed for each machine learning algorithm across different datasets. Table 5 presents the optimal results for each algorithm. Notably, all algorithms achieved results (Accuracy, F1 score, Recall, and Precision) exceeding 90%. KNN and RF emerged as the most effective algorithms for High Entropy Alloy (HEA) phase classification, boasting accuracies of 92.31% and 91.21%, respectively. Additionally, metrics such as F1 score, Recall, and Precision, as well as Cohen-Kappa score and Matthews Correlation Coefficient, recorded their highest values for KNN and RF classifiers, respectively. Furthermore, the losses (excluding Log loss) for KNN and RF were minimized compared to other algorithms [52].

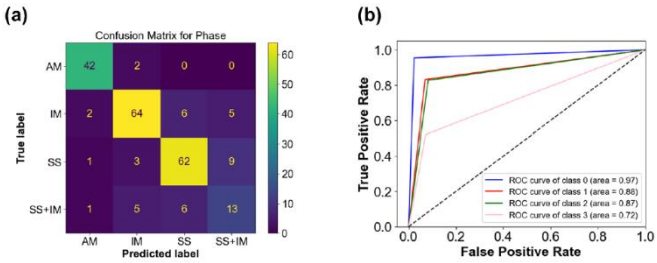

Figure 12. Assessment of the RF classifier utilizing (a) Confusion matrix, and (b) Receiver Operating Characteristic (ROC) curve for multi-scale data [53]

Multiclass classification in this study is conducted on a dataset comprising 36 features ranked in terms of significance. The primary aim of employing feature selection methodologies in this context is to reduce dataset dimensionality, enhance usability, and pinpoint the feature subset that yields optimal performance in overall classification [10]. The experimental procedure in this investigation encompasses five steps. Initially, the initial feature subset encompasses all 36 features of the dataset, serving as a control experiment. This subset is juxtaposed with elemental composition and other empirical parameter sets previously employed by Agarwal and Rao [33], Zhou et al. [34], and Wu et al. [55]. Subsequently, in the second stage, four feature-reduced ensembles are constructed through the implementation of LVQ, RF-RFE, SVM-RFE and Boruta algorithms for selecting features. In the third stage, features are systematically ranked based on their declining importance, with superior outcomes observed. Tables 6 and Table 7 reveal that the, SVM, ANN, KNN and RF classifiers have demonstrated superior performance compared to other utilized algorithms. Their rates of accuracy stand at 95.79%, 94.01%, 94.35%, and 97.48%, respectively. This dominance of SVM, ANN, KNN and RF, classifiers remain consistent across all feature ensembles. As noted by Ho and Tsai [56], "The overall accuracy of M1 will be notably high in scenarios where the test alloys exclusively pertain to [solid solution] alloys." In contrast, the NB and LDA classifiers exhibited lower performance, with accuracies ranging from 83% to 88%. Qu et al. [57] devised a method for phase identification in high-entropy alloys (HEAs) based on composition using machine learning tools. They employed the implementation of the Support Vector Machine (SVM) approach in forecast phase development in HEAs.

Table 5. Best performance of different ML algorithms on the oversampled dataset

ML Algorithms	Mean CV Accuracy (%)	Test Accuracy (%)	Precision (%)	F1 Score (%)	Recall (%)	Zero one loss (%)	Log loss	Hem loss (%)	Math Corr. (%)	CK Score (%)
SVM	84.40(±3.14)	90.11	90.11	90.08	90.11	9.9	0	9.9	85.2	85.1
RF	83.70(±2.24)	91.21	92.13	91.17	91.21	8.8	0.296	8.8	87.3	86.8
KNN	83.98(±2.20)	92.31	92.61	92.29	92.31	7.7	1.96	7.7	88.6	88.4
MLFFNN	85.91(±4.11)	90.66	91.46	90.57	90.66	9.3	0.291	9.3	86.5	86.0

Table 6. The accuracy of classification for various algorithms of machine learning in relation to diverse feature ensembles

ML Algorithms	Top 4 Ranked Features	Top 6 Ranked Features	Top 10 Ranked Features	Top 13 Ranked Features	Top 16 Ranked Features	Top 20 Ranked Features	Top 25 Ranked Features	All 36 Dataset Features
SVM	0.9376	0.9584	0.95843	0.9579	0.9574	0.9559	0.9499	0.9421
ANN	0.88759	0.90649	0.9347	0.9401	0.9278	0.9400	0.9273	0.9307
KNN	0.9300	0.8905	0.9431	0.9435	0.9138	0.9074	0.8732	0.889564
RF	0.96045	0.9678	0.9702	0.9748	0.9693	0.9718	0.9718	0.9693

Table 7. Kappa scores of various models corresponding to the number of selected features

ML Algorithms	Top 4 Ranked Features	Top 6 Ranked Features	Top 10 Ranked Features	Top 13 Ranked Features	Top 16 Ranked Features	Top 20 Ranked Features	Top 25 Ranked Features	All 36 Dataset Features
SVM	0.9465	0.9658	0.9703	0.9629	0.9688	0.9614	0.9554	0.9193
ANN	0.8655	0.9148	0.9283	0.9372	0.9462	0.9417	0.9327	0.9238
KNN	0.9495	0.9599	0.9539	0.9584	0.9316	0.9227	0.9287	0.9148
RF	0.9372	0.9552	0.9552	0.9896	0.9896	0.9896	0.9811	0.9552

Utilizing both the thermodynamic and composition parameters of HEAs, the researchers developed two SVM models. Both models demonstrated reliability exceeding 85%. Huang et al. [29] employed three distinct machine learning algorithms, namely Support Vector Machine (SVM), Artificial Neural Network (ANN) and K-Nearest Neighbor (KNN) to predict phases in high-entropy alloys (HEAs). The machine learning model effectively derived phase selection rules using an extensive empirical dataset encompassing 401 distinct HEAs, including 54 intermetallic compounds,174 solid solutions and 173 solid solutions with intermetallic phases. The architecture of the Multi-Layer Feed Forward Neural Network (MLFFNN) is depicted in Figure 5.

The accuracy rates for the, SVM, ANN and KNN models were 64.3%, 74.3% and 68.6%, respectively. Subsequently, the focus shifted to the categorization of two out of the three phases using ANN and SVM. Scatter plots depicting the average testing accuracy for various configurations of neurons within the three hidden layers revealed that ANN, in particular, achieved high accuracy values. For the classification of pairs of the three phases—intermetallic phases (IM), solid solution (SS), solid solution + intermetallic phases (SS+IM)—the testing accuracy values were 94.3%, 86.7%, and 78.9%, respectively. Consequently, the educated ANN model outperformed the other two machine learning models and proved advantageous for forecasting the phase of novel High-Entropy Alloys (HEAs).

5. Conclusions

This review paper provides an in-depth analysis of various methodologies employing machine learning (ML) techniques for accurately identifying phases in High Entropy Alloys (HEAs). It synthesizes research findings that highlight the efficacy of ML models in phase prediction, drawing attention to studies where models have achieved high accuracy levels, some validating their reliability with accuracy rates around 84%. A notable advancement discussed is the use of a voting ensemble, which combines several top-performing algorithms, resulting in improved prediction accuracies. The review emphasizes the importance of feature analysis in understanding the impact of different parameters on HEA phase determination. This analytical approach is not only instrumental in enhancing phase detection accuracy but also in advancing the broader understanding of material properties, aiding in the design of innovative materials for various applications. The paper also examines the utilization of alternative ML methods like K-Nearest Neighbor and Random Forest Classifier, which in some studies have achieved test accuracies exceeding 90%. These findings offer valuable contributions to the field of HEA phase prediction. Another critical aspect highlighted in this review is the importance of balanced datasets in model training. The studies reviewed demonstrate that well-curated datasets can significantly improve the accuracy of phase predictions, an essential factor considering the challenges and data scarcity inherent in the HEA domain. Looking ahead, the paper discusses future research directions, emphasizing the need for optimizing ML models for phase prediction in HEAs and the importance of collecting and generating comprehensive HEA datasets. These efforts are aimed at further enhancing the precision and reliability of predictive models. In conclusion, the review underscores the significant contributions of these studies to the design and predictive modeling of phases in novel High Entropy Alloys (HEAs) using advanced ML methods. The insights gathered from this comprehensive review are expected to guide future research and development in this rapidly evolving field of materials science.

Ethical issue

The authors are aware of and comply with best practices in publication ethics, specifically with regard to authorship (avoidance of guest authorship), dual submission, manipulation of figures, competing interests, and compliance with policies on research ethics. The authors adhere to publication requirements that the submitted work is original and has not been published elsewhere.

Data availability statement

The manuscript contains all the data. However, more data will be available upon request from the authors.

Conflict of interest

The authors declare no potential conflict of interest.

References

[1] J. Schmidt, M. R. G. Marques, S. Botti, and M. A. L. Marques, “Recent advances and applications of machine learning in solid-state materials science,” Npj Comput. Mater., vol. 5, no. 1, Art. no. 1, Aug. 2019, doi: 10.1038/s41524-019-0221-0.

[2] “Data-Driven Materials Science: Status, Challenges, and Perspectives - Himanen - 2019 - Advanced Science - Wiley Online Library.” Accessed: Dec. 21, 2023. [Online]. Available: https://onlinelibrary.wiley.com/doi/full/10.1002/advs.201900808

[3] D. Silver et al., “Mastering the game of Go with deep neural networks and tree search,” Nature, vol. 529, no. 7587, Art. no. 7587, Jan. 2016, doi: 10.1038/nature16961.

[4] “[1604.07316] End to End Learning for Self-Driving Cars.” Accessed: Dec. 21, 2023. [Online]. Available: https://arxiv.org/abs/1604.07316

[5] K. He, X. Zhang, S. Ren, and J. Sun, “Delving Deep into Rectifiers: Surpassing Human-Level Performance on ImageNet Classification,” presented at the Proceedings of the IEEE International Conference on Computer Vision, 2015, pp. 1026–1034. Accessed: Dec. 21, 2023. [Online]. Available: https://openaccess.thecvf.com/content_iccv_2015/html/He_Delving_Deep_into_ICCV_2015_paper.html

[6] S. Liu and Y. Tian, “Facial Expression Recognition Method Based on Gabor Wavelet Features and Fractional Power Polynomial Kernel PCA,” in Advances in Neural Networks - ISNN 2010, L. Zhang, B.-L. Lu, and J. Kwok, Eds., in Lecture Notes in Computer Science. Berlin, Heidelberg: Springer, 2010, pp. 144–151. doi: 10.1007/978-3-642-13318-3_19.

[7] M. Pazzani and D. Billsus, “Learning and Revising User Profiles: The Identification of Interesting Web Sites,” Mach. Learn., vol. 27, no. 3, pp. 313–331, Jun. 1997, doi: 10.1023/A:1007369909943.

[8] “A review of machine learning approaches to Spam filtering - ScienceDirect.” Accessed: Dec. 21, 2023. [Online]. Available: https://www.sciencedirect.com/science/article/abs/pii/S095741740900181X

[9] “Credit scoring with a data mining approach based on support vector machines - ScienceDirect.” Accessed: Dec. 21, 2023. [Online]. Available: https://www.sciencedirect.com/science/article/abs/pii/S095741740600217X

[10] R. Machaka, “Machine learning-based prediction of phases in high-entropy alloys,” Comput. Mater. Sci., vol. 188, p. 110244, Feb. 2021, doi: 10.1016/j.commatsci.2020.110244.

[11] M. Peters, J. Kumpfert, C. h. Ward, and C. Leyens, “Titanium Alloys for Aerospace Applications,” Adv. Eng. Mater., vol. 5, no. 6, pp. 419–427, 2003, doi: 10.1002/adem.200310095.

[12] R. Montanari, B. Riccardi, R. Volterri, and L. Bertamini, “Characterisation of plasma sprayed W coatings on a CuCrZr alloy for nuclear fusion reactor applications,” Mater. Lett., vol. 52, no. 1, pp. 100–105, Jan. 2002, doi: 10.1016/S0167-577X(01)00375-5.

[13] “Nanostructured High-Entropy Alloys with Multiple Principal Elements: Novel Alloy Design Concepts and Outcomes - Yeh - 2004 - Advanced Engineering Materials - Wiley Online Library.” Accessed: Dec. 21, 2023. [Online]. Available: https://onlinelibrary.wiley.com/doi/abs/10.1002/ad

em.200300567?casa_token=kY2yhmmuv-sAAAAA:HYOphDuSs_PiiOW6J7_87umuOt04W9ziz32YwXGfFVOgn3_-M2FnXjvQ_E4bgqV1artDbj2fhFYZd7nBtA

[14] "Enhanced strength and ductility in a high-entropy alloy via ordered oxygen complexes | Nature." Accessed: Dec. 21, 2023. [Online]. Available: https://www.nature.com/articles/s41586-018-0685-y

[15] M. C. Gao, J.-W. Yeh, P. K. Liaw, and Y. Zhang, High-Entropy Alloys: Fundamentals and Applications. Springer, 2016.

[16] "Rare-earth high-entropy alloys with giant magnetocaloric effect - ScienceDirect." Accessed: Dec. 21, 2023. [Online]. Available: https://www.sciencedirect.com/science/article/abs/pii/S1359645416309570

[17] Noor, Md Fahel Bin, Nusrat Yasmin, and Tiglet Besara. "Machine learning in high- entropy alloys: phase formation predictions with artificial neural networks." Future Sustainability 2, no. 1 (2024): 47-58.

[18] T.-T. Shun, C.-H. Hung, and C.-F. Lee, "The effects of secondary elemental Mo or Ti addition in Al0.3CoCrFeNi high-entropy alloy on age hardening at 700°C," J. Alloys Compd., vol. 495, no. 1, pp. 55–58, Apr. 2010, doi: 10.1016/j.jallcom.2010.02.032.

[19] Y. F. Ye, Q. Wang, J. Lu, C. T. Liu, and Y. Yang, "High-entropy alloy: challenges and prospects," Mater. Today, vol. 19, no. 6, pp. 349–362, Jul. 2016, doi: 10.1016/j.mattod.2015.11.026.

[20] Yasmin, Nusrat, Md Fahel Bin Noor, and Tiglet Besara. "Structure and Magnetism of the New Cage-structured Compound HfMn $ _ {2} $ Zn $ _ {20} $." arXiv preprint arXiv:2306.01146 (2023).

[21] B. Mallick, R. Das, S. Banik, Md.F. bin Noor, A. Habib, Performance Enhancement of an Automobile Radiator by Using a Nozzle Arrangement, International Journal of Innovative Technology and Exploring Engineering. X (2019).

[22] Md.F. bin Noor, B. Mallick, A. Habib, Heat storage system: A modern way to reuse and recycle energy to reduce thermal pollution, in: International Conference on Mechanical, Industrial and Energy Engineering, 2018.

[23] Md.F. bin Noor, Md.A.M. Hossain, B. Mallick, A. Habib, Experimental Evaluation with Comparative Steady-State Thermal Analysis of Two-Wheeler Engine Cylinder by Varying Its Material, in: International Conference on Mechanical Engineering and Renewable Energy, 2019.

[24] A. Habib, M. Bhuiya, Md.F. bin Noor, B. Mallick, Biodiesel Production from Castor Seed Oil as an Alternative Fuel for the Compression Ignition (Ci) Engine, in: International Conference on Mechanical Engineering and Renewable Energy, 2019.

[25] Yasmin, Nusrat, Md Fahel Bin Noor, and Tiglet Besara. "Exploring Single Crystals as Promising Thermoelectric Materials." Bulletin of the American Physical Society (2023).

[26] Noor, Md Fahel Bin, Nusrat Yasmin, and Tiglet Besara. "The Exploration and Synthesisof Two Intermetallic Single Crystals." Bulletin of the American Physical Society (2023).

[27] Noor, Md Fahel Bin, Nusrat Yasmin, and Tiglet Besara. "Synthesis and Exploration of Heusler Intermetallics as Potential Catalysts." Bulletin of the American Physical Society (2023).

[28] Yasmin, Nusrat, Md Fahel Bin Noor, Sarah Longworth, and Tiglet Besara. "Synthesis of Cage-structured Compounds for Thermoelectricity." Bulletin of the American Physical Society (2023).

[29] W. Huang, P. Martin, and H. L. Zhuang, "Machine-learning phase prediction of high-entropy alloys," Acta Mater., vol. 169, pp. 225–236, May 2019, doi: 10.1016/j.actamat.2019.03.012.

[30] L. Qiao, Y. Liu, and J. Zhu, "A focused review on machine learning aided high-throughput methods in high entropy alloy," J. Alloys Compd., vol. 877, p. 160295, Oct. 2021, doi: 10.1016/j.jallcom.2021.160295.

[31] N. Islam, W. Huang, and H. L. Zhuang, "Machine learning for phase selection in multi-principal element alloys," Comput. Mater. Sci., vol. 150, pp. 230–235, Jul. 2018, doi: 10.1016/j.commatsci.2018.04.003.

[32] D. B. Miracle and O. N. Senkov, "A critical review of high entropy alloys and related concepts," Acta Mater., vol. 122, pp. 448–511, Jan. 2017, doi: 10.1016/j.actamat.2016.08.081.

[33] A. Agarwal and A. K. Prasada Rao, "Artificial Intelligence Predicts Body-Centered-Cubic and Face-Centered-Cubic Phases in High-Entropy Alloys," JOM, vol. 71, no. 10, pp. 3424–3432, Oct. 2019, doi: 10.1007/s11837-019-03712-4.

[34] Z. Zhou, Y. Zhou, Q. He, Z. Ding, F. Li, and Y. Yang, "Machine learning guided appraisal and exploration of phase design for high entropy alloys," Npj Comput. Mater., vol. 5, no. 1, Art. no. 1, Dec. 2019, doi: 10.1038/s41524-019-0265-1.

[35] D. Morgan and R. Jacobs, "Opportunities and Challenges for Machine Learning in Materials Science," Annu. Rev. Mater. Res., vol. 50, no. 1, pp. 71–103, 2020, doi: 10.1146/annurev-matsci-070218-010015.

[36] C. J. Stone, "Consistent Nonparametric Regression," Ann. Stat., vol. 5, no. 4, pp. 595–620, 1977.

[37] "An Introduction to Kernel and Nearest-Neighbor Nonparametric Regression: The American Statistician: Vol 46, No 3." Accessed: Dec. 22, 2023. [Online]. Available: https://www.tandfonline.com/doi/abs/10.1080/00031305.1992.10475879

[38] "k-Nearest Neighbor Classification | SpringerLink." Accessed: Dec. 22, 2023. [Online]. Available: https://link.springer.com/chapter/10.1007/978-0-387-88615-2_4

[39] "Euclidean distance mapping - ScienceDirect." Accessed: Dec. 22, 2023. [Online]. Available: https://www.sciencedirect.com/science/article/abs/pii/0146664X80900544

[40] P. Guillen, M. Robinson, C. Torres, and E. Pereya, "Support Vector Machine Application for Multiphase Flow Pattern Prediction," Jun. 2018. doi: 10.48550/arXiv.1806.05054.

[41] A. Shmilovici, "Support Vector Machines," in Data Mining and Knowledge Discovery Handbook, O. Maimon and L. Rokach, Eds., Boston, MA: Springer US, 2010, pp. 231–247. doi: 10.1007/978-0-387-09823-4_12.

[42] "(PDF) Wavelet Support Vector Machine." Accessed: Dec. 22, 2023. [Online]. Available: https://www.researchgate.net/publication/8345770_Wavelet_Support_Vector_Machine

[43] B. M. H. Romeny, Front-End Vision and Multi-Scale Image Analysis: Multi-scale Computer Vision Theory and Applications, written in Mathematica. Springer Science & Business Media, 2008.

[44] E. Byvatov, U. Fechner, J. Sadowski, and G. Schneider, "Comparison of Support Vector Machine and Artificial Neural Network Systems for Drug/Nondrug Classification," J. Chem. Inf. Comput. Sci., vol. 43, no. 6, pp. 1882–1889, Nov. 2003, doi: 10.1021/ci0341161.

[45] S. N. Sivanandam, "Introduction to neural networks using MATLAB 6.0," No Title, Accessed: Dec. 22, 2023. [Online]. Available: https://cir.nii.ac.jp/crid/1130282272202172160

[46] K. Hornik, "Approximation capabilities of multilayer feedforward networks," Neural Netw., vol. 4, no. 2, pp. 251–257, Jan. 1991, doi: 10.1016/0893-6080(91)90009-T.

[47] "On the Optimality of the Simple Bayesian Classifier under Zero-One Loss | Machine Learning." Accessed: Dec. 24, 2023. [Online]. Available: https://link.springer.com/article/10.1023/A:1007413511361

[48] E. Alpaydin, Introduction to Machine Learning, fourth edition. MIT Press, 2020. ISBN: 9780262043793

[49] L. Breiman, "Random Forests," Mach. Learn., vol. 45, no. 1, pp. 5–32, Oct. 2001, doi: 10.1023/A:1010933404324.

[50] L. Breiman, "CONSISTENCY FOR A SIMPLE MODEL OF RANDOM FORESTS," 2004. Accessed: Dec. 24, 2023. [Online]. Available: https://www.semanticscholar.org/paper/CONSISTENCY-FOR-A-SIMPLE-MODEL-OF-RANDOM-FORESTS-Breiman/2a42f39add8332a7139d44a6e77496c0571e4f24

[51] Y. Lin and Y. Jeon, "Random Forests and Adaptive Nearest Neighbors," J. Am. Stat. Assoc., vol. 101, no. 474, pp. 578–590, 2006.

[52] S. Risal, W. Zhu, P. Guillen, and L. Sun, "Improving phase prediction accuracy for high entropy alloys with Machine learning," Comput. Mater. Sci., vol. 192, p. 110389, May 2021, doi: 10.1016/j.commatsci.2021.110389.

[53] T. Nazir, N. Shaukat, N. ul H. Tariq, R. N. Shahid, and M. H. Bhatti, "A comprehensive strategy for phase detection of high entropy alloys: Machine learning and deep learning approaches," Mater. Today Commun., vol. 37, p. 107525, Dec. 2023, doi: 10.1016/j.mtcomm.2023.107525.

[54] F. Sustainability, "Machine learning in high-entropy alloys: phase formation predictions with artificial neural networks | Future Sustainability," Dec. 2023, Accessed: Dec. 27, 2023. [Online]. Available: https://fupubco.com/fusus/article/view/147

[55] "Uncovering the eutectics design by machine learning in the Al–Co–Cr–Fe–Ni high entropy system - ScienceDirect." Accessed: Dec. 27, 2023. [Online]. Available: https://www.sciencedirect.com/science/article/abs/pii/S1359645419307050

[56] "Theories for predicting simple solid solution high-entropy alloys: Classification, accuracy, and important factors impacting accuracy - ScienceDirect." Accessed: Dec. 27, 2023. [Online]. Available: https://www.sciencedirect.com/science/article/abs/pii/S1359646220304322

[57] N. Qu, Y. Chen, Z. Lai, Y. Liu, and J. Zhu, "The phase selection via machine learning in high entropy alloys," Procedia Manuf., vol. 37, pp. 299–305, Jan. 2019, doi: 10.1016/j.promfg.2019.12.051.